Supercurrent distribution in high-T_C superconducting $YBa_2Cu_3O_{7-y}$ thin films by scanning superconducting quantum interference device microscopy

Akira Sugimoto, Tetsuji Yamaguchi, and Ienari Iguchi[a)]
Department of Physics and CREST-JST, Tokyo Institute of Technology, 2-12-1 Oh-okayama, Meguro-ku, Tokyo 152-8551, Japan

(Received 31 July 2000; accepted for publication 6 September 2000)

The two-dimensional vector mapping of current distributions in high-T_C superconducting $YBa_2Cu_3O_{7-y}$ thin films obtained by converting magnetic-field data measured by scanning superconducting quantum interference device (SQUID) microscopy is reported. The current distribution contains the contributions from both transport supercurrent and vortex current. The transport supercurrent is found to flow mainly along the edge of a stripline, and the numerical calculation based on the simple London model by taking the specific sample-detector geometry into account is given. The agreement between the experimental data and the calculated results is good, demonstrating that the scanning SQUID microscope provides a useful tool for studying the current distribution in a superconductor. © *2000 American Institute of Physics.* [S0003-6951(00)03145-4]

The applications of superconducting quantum interference devices (SQUIDs) have been recently developing remarkably. Particularly, the scanning SQUID microscope (SSM) has been found to be very profitable for various applications such as nondestructive evaluation of steels,[1] the detection of magnetostatic bacteria,[2] and the other magnetic materials at room temperature[3] because of high magnetic sensitivity and spatial resolution. It is also useful for observing the trapped vortices in the circuit of Nb electronic devices[4] and the high-T_C $YBa_2Cu_3O_{7-y}$(YBCO) single crystal[5] at low temperature. The SSM technique also gave proof of *d*-wave symmetry of high-T_C superconductor by observing the half-flux quantum $\Phi_0/2$, ($\Phi_0 \simeq 2.07 \times 10^{-15}$ Wb) at a YBCO tricrystal junction boundary.[6] It has been pointed out that the SSM can also probe a current distribution by use of the inverted Biot–Savart law. Wellstood and co-workers[7] obtained the current distribution of a semiconductor chip at room temperature by measuring the spatial distribution of magnetic field using a SSM. While the magneto-optical imaging,[8,9] Hall-probe,[9] and the THz-mapping[10] techniques are also useful methods to observe the current distribution in a superconductor, their sensitivity is much lower than SSM and a single vortex current cannot be resolved using these techniques.

In this letter, we report the supercurrent distribution of a YBCO thin film in the presence of both the quantized vortices and the transport current using the SSM. The observed magnetic signal is converted into the current distribution by the inverted Biot–Savart law. The results are in good qualitative agreement with the calculated ones using the simple London model.

We used a scanning SQUID microscope system almost similar to that of Ref. 4. It contains a dc-SQUID magnetometer made of Nb/Al–AlO_x/Nb tunnel Josephson junctions fabricated on a 3×3 mm^2 Si chip. The magnetometer had a one-turn pickup coil of 10 μm diameter, and was located 45 μm apart from the edge of the chip. The sample-coil distance was about 10 μm and the magnetic flux sensitivity was better than $5\mu\Phi_0/\sqrt{\text{Hz}}$. The cryostat system used here was equipped with two Cu-cold head stages cooled by helium gas, one as a SQUID holder, the other as a sample stage. The sample temperature was controllable between 4 and 100 K by a dc current heater and control of helium gas flow. A Cu wire coil was wound around the sample holder to generate a small magnetic field. The *xyz* stage with stepping motors and the SQUID were controlled by a personal computer, and the magnetic-field signal was recorded.

YBCO thin films were deposited by a pulsed laser deposition method. The film thickness was about 100 nm. All samples were patterned by conventional photolithography and the Ar ion milling technique. The width of a YBCO stripline was 20–100 μm. The critical temperature (T_C) was around 88 K, and the current density (J_C) was about 10^7 A/cm^2 at 10 K.

The SSM signals were recorded as the two-dimensional (2D) distribution map of the *z* component of the magnetic field. From these data, the local current distribution, including its magnitude and direction, was derived by solving the Biot–Savart law according to the work by Wikswo and co-workers.[11] The Biot–Savart law in Fourier space is given by

$$b_z(k_x,k_y)=\frac{i\mu_0 d}{2}\,\frac{e^{-kz_0}}{k}\,[k_y j_x(k_x,k_y)-k_x j_y(k_x,k_y)], \tag{1}$$

where, b_z is the 2D Fourier transform of magnetic field $B_z(x,y)$, j_x and j_y are also Fourier transforms of current density $J_x(x,y)$ and $J_y(x,y)$, respectively, k_x and k_y are the spatial frequencies in *x* and *y* directions, $k=\sqrt{k_x^2+k_y^2}$, μ_0 is the permeability of free space, *d* is the film thickness of the sample, and z_0 is the SQUID-sample separation distance. Equation (1) holds for the condition $z_0 \gg d$, which is satisfied

a)Electronic mail: iguchi@ap.titech.ac.jp

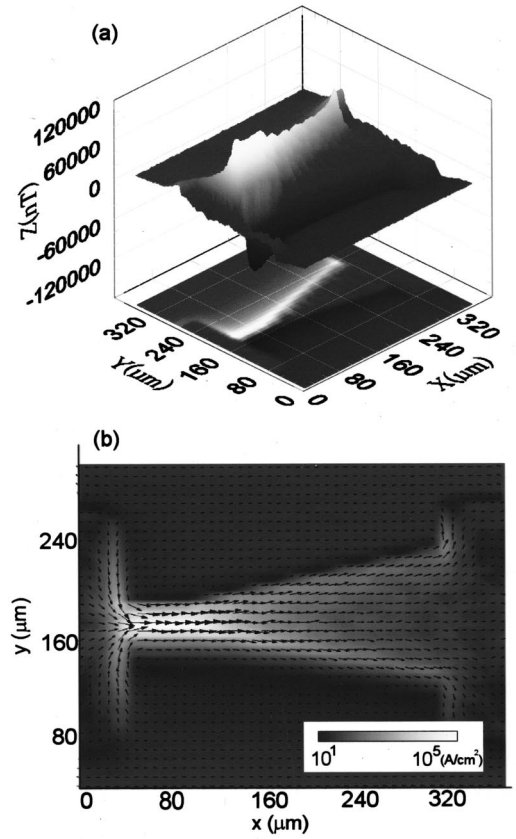

FIG. 1. (a) Magnetic-field image of a wedge-shaped YBCO thin film in the presence of transport current (5.0 mA). (b) Calculated current distribution and current vector. The length of each arrow indicates the amplitude of current density.

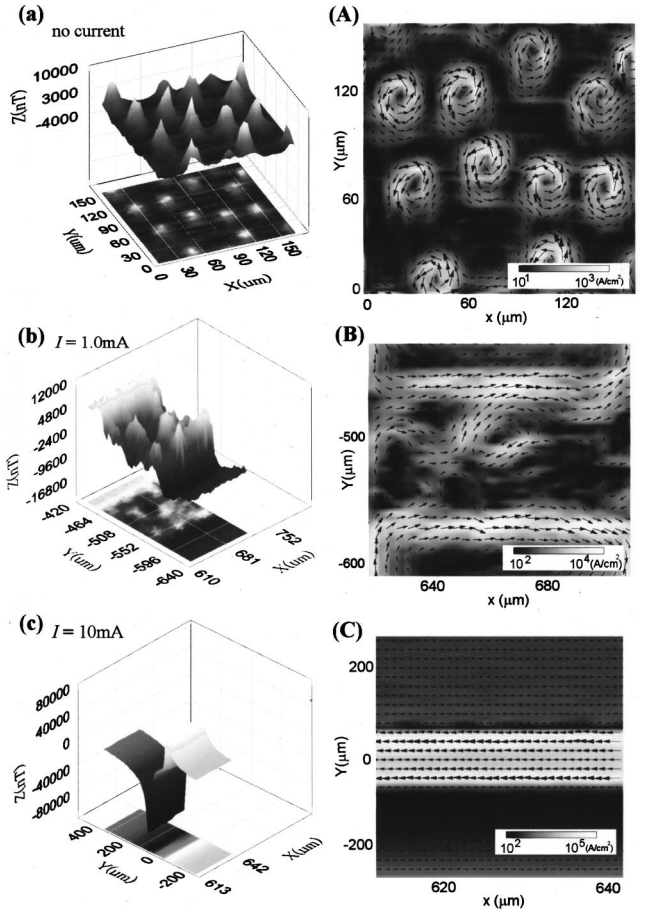

FIG. 2. (a) Observed vortex structure in the absence of transport current in a YBCO film. (A) Calculated current distribution and current vector from Fig. 2(a). (b) Observed magnetic-field image of the YBCO thin film with 100 μm width in the presence of transport current (1.0 mA) and a trapped vortex. (B) The calculated current distribution from Fig. 2(b). (c) Observed magnetic-field image of the same sample as in Fig. 2(b) under different transport current (10 mA). (C) The calculated current distribution from Fig. 2(c).

with our experimental geometry. By combining Eq. (1) with the Fourier transformed equation of continuity

$$-ik_x j_x(k_x,k_y)-ik_y j_y(k_x,k_y)=0, \tag{2}$$

we obtain

$$j_x=-\frac{2i}{\mu_0 d}\frac{e^{kz_0}}{k}k_y b_z(k_x,k_y), \tag{3}$$

$$j_y=\frac{2i}{\mu_0 d}\frac{e^{kz_0}}{k}k_x b_z(k_x,k_y). \tag{4}$$

J_x and J_y are obtained by inverse Fourier transformation of Eqs. (3) and (4). In practice, at first, the magnetic-field data are converted into fast Fourier transform (FFT), then j_x and j_y are calculated using Eqs. (3) and (4) in k space, and finally, J_x and J_y are obtained by inverse FFT of j_x and j_y. The proper cutoff frequency (low-pass frequency, k_w) in k space is necessary if B_z data contain some periodical noise.[7]

Figure 1 shows the observed SSM image data of a wedge-shaped YBCO thin film in the presence of transport current. The widest width was about 100 μm, and the narrowest width was about 20 μm. Figure 1(a) is the magnetic-field distribution of this sample, and Figure 1(b) is the calculated current distribution. The length of each arrow indicates the amplitude of current density. One sees that supercurrent in the wide section tends to flow along the edge part of a stripline, while in the narrow section (20 μm), it was not visible because of limited spatial resolution ($\sim$10 μm).

Figures 2(a) and 2(A) show the observed vortex structure and the calculated supercurrent distribution in the absence of transport current in a YBCO thin film. The vortices appeared randomly distributed and the supercurrents associated with these vortices were circular, as expected. The magnetic flux for each vortex was estimated to be $(2.00\pm0.1)\times10^{-15}$ Wb, in good agreement with one flux quantum value $\Phi_0=2.07\times10^{-15}$ Wb. Figure 2(b) and 2(c) show the observed magnetic-field images of the YBCO thin film with 100 μm width, and the corresponding current distributions for different transport currents (1.0 and 10 mA) are given in Figs. 2(B) and 2(C), respectively. In Fig. 2(b), the magnetic-field data contain a single trapped vortex, hence the current distribution consists of the sum of transport current and vortex shielding current. The transport current flows mainly along the edge of the stripline, and small circular current that generates the vortex is also seen in the center part of this image. By considering the spread of a magnetic field at the detecting position (about 10 μm height above the sample surface) and the pickup coil of 10 μm ϕ, the real vortex and transport currents would be localized in a small area. In Fig. 2(B), the calculated current image in left- and right-hand sides showed ''edge effect'' of Gibb's phenomena. This ef-

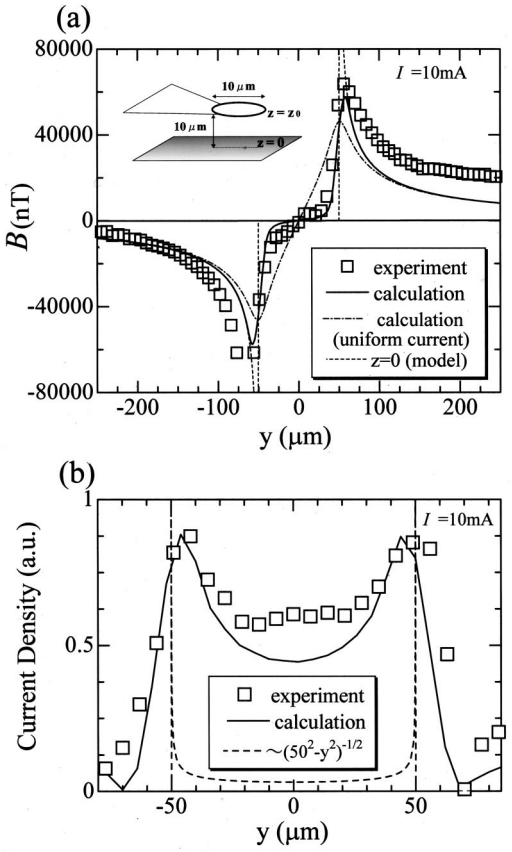

FIG. 3. (a) Open square dots are the magnetic-field data across the film ($x=635\ \mu$m) of Fig. 2(c). The dashed line is the sample surface ($z=0$) distribution given by Eq. (5). The solid line is the calculated curve by assuming Eq. (5) and taking the detection area of the pickup loop and the SQUID-sample separation distance into account (see the inset). The dash-dotted line is the magnetic field by assuming a uniform current. (b) Open square dots are the experimental data of current density across the film of Fig. 2(C). The solid line is the calculated current distribution based on $B(x,y,z_0)$. The dashed line is the current distribution model on the surface.

fect inevitably comes in as long as Fourier transformation is used. In Figs. 2(c) and 2(C), the results seemed to show only transport current. Since the current value (10 mA) was ten times larger than that of Figs. 2(b) and 2(B), we judge that vortex current was buried in this large current background and not observable.

Figures 3(a) and 3(b) show the magnetic-field data and the calculated current distribution across the film of Figs. 2(c) and 2(C), together with numerical results based on the simple London model. Since the transport current was only 1% of film critical current ($\sim$1 A), we assume the most ideal and classical model[12–14] $J(y)=I(a^2-y^2)^{-1/2}/\pi$ in all but the extreme edge regions, where a is the half-width of stripline. The magnetic field is given by

$$B(y)=\begin{cases} 0 & (|y|<a) \\ \dfrac{\mu_0 I}{2\pi}\dfrac{y/|y|}{\sqrt{y^2-a^2}} & (|y|>a). \end{cases} \tag{5}$$

The calculated $B(y)$ and $J(y)$ profiles correspond to the dashed lines in Figs. 3(a) and 3(b), respectively. The solid line in Fig. 3(a) is the calculated curve of a magnetic-field distribution at the detector position by assuming that the surface ($z=0$) distribution is given by Eq. (5) and was obtained by the following procedure. First, the extended 2D distribution data of $B(x,y,z=0)$ [Eq. (5)] was transformed into $b(k_x,k_y,z=0)$ by FFT, then we obtained the magnetic-field data at $z=z_0$ by the relation $b(k_x,k_y,z_0)=e^{kz_0}b(k_x,k_y,z=0)$ in the k space. $B(x,y,z_0)$ was obtained by inverse Fourier transformation of $b(k_x,k_y,z_0)$. Since the SQUID pickup coil had 10 μm circular shape, the integration $B(x,y,z_0)$ was performed over this circle area. The open square dots are experimental data. The agreement between the experimental data and the calculated result is qualitatively good. In the case where the transport current flows uniformly in the stripline, the magnetic profile exhibits steep slope around $y=0\ \mu$m (dash-dotted line), in disagreement with the experimental result. For $100\ \mu\text{m}<y<200\ \mu$m, the discrepancy occurred due to the slight tilt of SQUID pickup coil to the y direction.

The solid line in Fig. 3(b) is the calculated current distribution based on $B(x,y,z_0)$. Open square dots were obtained from the experimental magnetic-field data in Fig. 3(a), and the dashed line is the current distribution model on the surface as obtained from Eq. (5). The experimental current distribution almost agrees with the calculated result by taking the detection area of the SQUID loop into account. Although the 2D mapping of current distribution does not exactly correspond to that of real surface ($z=0$) itself, it essentially reflects the true nature of transport current or vortex current demonstrating that this method provides a powerful tool for obtaining the current distribution in many electronic specimens.

In summary, we have investigated supercurrent distribution in the presence of both transport current and vortex current in a YBCO thin film by numerically converting the magnetic-field data observed by a scanning SQUID microscope. The transport supercurrent was found to flow mainly along the edge of a stripline, and the comparison was made with the simple London model. This method can be applied to the study of current distribution in various kinds of devices or specimens.

[1] T. J. Shaw, K. Schlenga, R. McDermott, J. Clarke, J. W. Chan, S. H. Kang, and J. W. Morris, Jr., IEEE Trans. Appl. Supercond. **9**, 4107 (1999).
[2] T. S. Lee, Y. R. Chemla, E. Dantsker, and J. Clarke, IEEE Trans. Appl. Supercond. **7**, 3247 (1997).
[3] J. Dechert, M. Mueck, and C. Heiden, IEEE Trans. Appl. Supercond. **9**, 4111 (1999).
[4] T. Morooka, S. Nakayama, A. Odawara, and K. Chinone, Jpn. J. Appl. Phys., Part 2 **38**, L119 (1999).
[5] K. A. Moler, J. R. Kirtley, R. Liang, D. Bonn, and W. N. Hardy, Phys. Rev. B **55**, 12753 (1997).
[6] J. R. Kirtley, C. C. Tsuei and K. A. Moler, Science **285**, 1373 (1999).
[7] E. F. Fleet, S. Chatraphorn, and F. C. Wellstood, IEEE Trans. Appl. Supercond. **9**, 4103 (1999).
[8] Ch. Jooss, R. Warthmann, A. Forkl, and H. Kronmüller, Physica C **299**, 215 (1998).
[9] P. D. Grant, M. W. Denhoff, W. Xing, P. Brown, S. Govorkov, J. C. Irwin, B. Heinrich, H. Zhou, A. A. Fife, and A. R. Cragg, Physica C **229**, 289 (1994).
[10] O. Morikawa, M. Yamashita, H. Saijo, M. Morimoto, M. Tonouchi, and M. Hangyo, Appl. Phys. Lett. **75**, 3387 (1999).
[11] B. J. Roth, N. G. Sepulveda, and J. P. Wikswo, Jr., J. Appl. Phys. **65**, 361 (1989).
[12] E. H. Rhoderick and E. M. Wilson, Nature (London) **194**, 1167 (1962).
[13] E. H. Brandt and M. Indenbom, Phys. Rev. B **48**, 12893 (1993).
[14] E. H. Brandt, Z. Phys. B: Condens. Matter **80**, 167 (1990) [Eq. (30)].